THE JOURNAL OF BIOLOGICAL CHEMISTRY VOL. 283, NO. 52, pp. 36416–36424, December 26, 2008

Analysis of Glucose Transporter Topology and Structural Dynamics*

Received for publication, June 24, 2008, and in revised form, October 6, 2008 Published, JBC Papers in Press, November 3, 2008, DOI 10.1074/jbc.M804802200

David M. Blodgett, Christopher Graybill, and Anthony Carruthers[1]

From the Department of Biochemistry and Molecular Pharmacology, University of Massachusetts Medical School, Worcester, Massachusetts 01605

Homology modeling and scanning cysteine mutagenesis studies suggest that the human glucose transport protein GLUT1 and its distant bacterial homologs LacY and GlpT share similar structures. We tested this hypothesis by mapping the accessibility of purified, reconstituted human erythrocyte GLUT1 to aqueous probes. GLUT1 contains 35 potential tryptic cleavage sites. Fourteen of 16 lysine residues and 18 of 19 arginine residues were accessible to trypsin. GLUT1 lysine residues were modified by isothiocyanates and *N*-hydroxysuccinimide (NHS) esters in a substrate-dependent manner. Twelve lysine residues were accessible to sulfo-NHS-LC-biotin. GLUT1 trypsinization released full-length transmembrane helix 1, cytoplasmic loop 6–7, and the long cytoplasmic C terminus from membranes. Trypsin-digested GLUT1 retained cytochalasin B and D-glucose binding capacity and released full-length transmembrane helix 8 upon cytochalasin B (but not D-glucose) binding. Transmembrane helix 8 release did not abrogate cytochalasin B binding. GLUT1 was extensively proteolyzed by α-chymotrypsin, which cuts putative pore-forming amphipathic α-helices 1, 2, 4, 7, 8, 10, and 11 at multiple sites to release transmembrane peptide fragments into the aqueous solvent. Putative scaffolding membrane helices 3, 6, 9, and 12 are strongly hydrophobic, resistant to α-chymotrypsin, and retained by the membrane bilayer. These observations provide experimental support for the proposed GLUT1 architecture; indicate that the proposed topology of membrane helices 5, 6, and 12 requires adjustment; and suggest that the metastable conformations of transmembrane helices 1 and 8 within the GLUT1 scaffold destabilize a sugar translocation intermediate.

The major facilitator superfamily (MFS)[2] of transport proteins comprises more than 1,000 proteins that mediate passive and secondary active transfer of small molecules across membranes (1). The facilitative glucose transport proteins (GLUT1–12) catalyze monosaccharide uniport in vertebrates (2) and display tissue-specific isoform expression. GLUT1 is expressed in most tissues but is especially abundant in the circulatory system (3) and at blood-tissue barriers such as the blood-brain barrier (4).

GLUT1 comprises 492 amino acids; is hydrophobic; contains a single, exofacial *N*-linked glycosylation site (5); and is predominantly α-helical (6). Hydropathy analysis (5), scanning glycosylation mutagenesis (7), proteolysis, antibody binding, and covalent modification studies indicate that GLUT1 contains intracellular N and C termini and 12 transmembrane domain (TM) α-helices (8). Amphipathic α-helices are proposed to form an aqueous translocation pathway for glucose transport across the plasma membrane (9–11). However, the detailed three-dimensional structure of GLUT1 is not known, and GLUT1 conformational changes catalyzing transport are unclear.

The structures of bacterial MFS transport proteins offer new insights into carrier structure (12). The lactose permease (LacY (13)), the glycerol 3-phosphate antiporter (GlpT (14)), a multidrug transporter (EmrD (15)), and the oxalate transporter (OxlT (16)) display little sequence similarity but share similar structures suggesting a common MFS protein architecture. Although mammalian MFS proteins, such as GLUT1, can be refractory to three-dimensional crystallization (12, 17), they may be homology-modeled using crystallized homologs as templates (12).

Salas-Burgos *et al.* (11) and Holyoake *et al.* (18) have modeled a GLUT1 structure using the GlpT template and biochemical and mutagenesis data to validate their results. GLUT1 cysteine-scanning mutagenesis studies (10) broadly support the resulting GLUT1 MFS α-helical packing arrangement but also note significant accessibility in TM regions that, according to the model, should be inaccessible (10). Docking analysis of cytochalasin B (a transport inhibitor) binding to homology-modeled GLUT1 positions the binding site within the cytoplasmic loop linking TMs 2 and 3 (11), whereas biochemical studies suggest that cytochalasin B binds close to cytoplasmic loop 10–11 (19–21). This discrepancy is consistent with a recent demonstration

* This work was supported, in whole or in part, by National Institutes of Health Grants DK44888 and DK36081. This work was also supported by American Diabetes Association Grant 1-06-IN-04 (Gail Patrick Innovation Award supported by a generous gift from the Estate of Gail Patrick).The costs of publication of this article were defrayed in part by the payment of page charges. This article must therefore be hereby marked "*advertisement*" in accordance with 18 U.S.C. Section 1734 solely to indicate this fact.

[1] To whom correspondence should be addressed: Dept. of Biochemistry and Molecular Pharmacology, University of Massachusetts Medical School, 364 Plantation St., Worcester, MA 01605. Tel.: 508-856-5570; E-mail: anthony.carruthers@umassmed.edu.

[2] The abbreviations used are: MFS, major facilitator superfamily; C-Ab, rabbit polyclonal antiserum raised against a synthetic peptide comprising GLUT1 residues 480–492; CB, cytochalasin B; DMSO, dimethylsulfoxide; ELISA, enzyme-linked immunosorbent assay; EmrD, the multidrug transporter of *Escherichia coli*; GlpT, glycerol 3-phosphate glycerol antiporter of *E. coli*; GLUT1, human erythrocyte glucose transport protein; LacY, the lactate:proton symporter of *E. coli*; MS, mass spectrometry; OxlT, oxalate transport of *Oxalobacter formigenes*; RhD, Rh blood group D antigen; HPLC, high performance liquid chromatography; ESI, electrospray ionization; sulfo-NHS-LC-biotin, sulfosuccinimidyl-6-(biotinamido)hexanoate; TM, transmembrane domain; NHS, *N*-hydroxysuccinimide; L, loop.

that homology modeling approximates carrier topology and architecture but is less successful at defining the spatial arrangement of specific residues (22). Deviations between experimental and modeled structures may also reflect structural and functional differences between template and target proteins.

The proposed GLUT1 architecture is inherently accessible to experimental evaluation. GLUT1 contains 16 lysine and 20 arginine residues (5) located within proposed intra- and extracellular loops, within the N and C termini, and at the membrane/solvent interface. Water-exposed lysine residues should be accessible to primary amine-reactive, polar covalent probes. Water-exposed lysine and arginine residues may also be accessible to trypsin. This study examined the accessibility of membrane-resident GLUT1 to proteases and to primary amine-reactive covalent probes. To maximize *in vivo* relevance, we specifically studied human erythrocyte GLUT1 purified under conditions where native function and quaternary structure are preserved (23). Our findings provide direct experimental support for the proposed GLUT1 architecture, suggest that the topology of some membrane helices requires minor adjustment, and illustrate that transmembrane helix 8 undergoes significant conformational change upon GLUT1 ligand binding.

EXPERIMENTAL PROCEDURES

Materials—Fresh, de-identified human blood was from Biological Specialties Corp. (Colmar, PA). Protein assays, Pro Blue Coomassie stain, sulfo-NHS-LC-biotin, fluorescein isothiocyanate, and SuperSignal chemiluminescence kits were from Pierce. Glycerol-free endoglycosidase peptide-*N*-glycosidase F was from New England Biolabs (Ipswich, MA). Nitrocellulose and Immobilon-P were from Fisher Scientific. Purified rabbit IgGs raised against a synthetic cytoplasmic C-terminal peptide of human GLUT1 (C-Ab, residues 480–492) were from Animal Pharm Services, Inc. (Healdsburg, CA). All other reagents were from Sigma-Aldrich.

Solutions—Saline comprised 150 mM NaCl, 10 mM Tris-HCl, and 0.5 mM EDTA, pH 7.4. Lysis medium contained 10 mM Tris-HCl and 0.2 mM EDTA, pH 7.2. Tris medium contained 50 mM Tris-HCl, pH 7.4. Kaline consisted of 150 mM KCl, 5 mM HEPES, 4 mM EGTA, and 5 mM $MgCl_2$. Phosphate-buffered saline containing Tween comprised 140 mM NaCl, 10 mM Na_2HPO_4, 3.4 mM KCl, 1.84 mM KH_2PO_4, and 0.1% Tween, pH 7.3.

Human Erythrocyte Membranes and Glucose Transport Protein—Glucose transporter and endogenous lipids were purified from human erythrocyte membranes in the absence of reductant as described previously (24, 25). The resulting unsealed GLUT1 proteoliposomes (26) contain 90% GLUT1, 8% RhD protein, and 2% nucleoside transporter (by protein mass) and contain equal masses of lipid and protein (27).

Cytochalasin B Binding—[^{3}H]cytochalasin B (CB) binding to GLUT1 proteoliposomes was measured as described previously (23).

GLUT1 Deglycosylation—GLUT1 (50 μg in 50 μl of kaline buffer) was incubated with 1,500 activity units of peptide-*N*-glycosidase F for 1 h at 37 °C.

Gel Electrophoresis and Western Blotting—GLUT1 protein was resolved on 8% polyacrylamide gels (28). Immunoblot analysis used C-Ab at 1:10,000 dilution as described previously (27).

GLUT1 Covalent Modification—GLUT1 (25–100 μg) was incubated with EZ-Link sulfo-NHS-LC-biotin (10 mM; pH 7.4, 4 °C), with fluorescein isothiocyanate (500 μM; pH 8, 4 °C), or with [^{14}C]phenylisothiocyanate (50 μM; pH 8.0, 4 °C) at GLUT1:covalent probe molar ratios ranging from 1:0.2 to 1:2,000 for 1 min to 1,800 min (29). Reactions were quenched with 50 mM Tris-HCl or glycine, and membranes were sedimented, washed several times with additional quench solution, and resuspended in medium appropriate for follow-up analysis.

ELISA—Biotin incorporation was quantitated by ELISA. Wells were precoated with C-Ab (200 μl of a 1:5,000 dilution; 300 min at 37 °C) and then blocked with 3% bovine serum albumin (120 min at 37 °C). Biotinylated GLUT1 was solubilized (2% Triton X-100 in phosphate-buffered saline for 60 min at 4 °C), clarified by centrifugation ($\approx$200,000 $\times$ *g* for 15 min), and applied to triplicate wells (200 μl/well, 2-h incubation at 4 °C). Wells were washed and blocked in phosphate-buffered saline containing 3% bovine serum albumin and 2% Triton X-100. Horseradish peroxidase-conjugated streptavidin was added (1 μg/ml; 1 h at 20 °C), and following washing, product development was measured as absorbance at 415 nm using a Benchmark Microplate Reader (Bio-Rad).

Tryptic and α-Chymotryptic Digested GLUT1 Peptides—Unmodified or pretreated reconstituted GLUT1 in kaline (0.5 mg/ml, 55-μl total reaction volume) was digested with trypsin or α-chymotrypsin at a 1:10 ratio (enzyme:GLUT1 by mass) for 0–2 h at 30 °C. Peptides were subjected to HPLC-ESI-MS/MS immediately or were processed further. Digests were separated into aqueous and membrane fractions by centrifugation for 30 min at 4 °C in a Beckman air-driven ultracentrifuge ($\approx$200,000 $\times$ *g*).

HPLC Separation of GLUT1 Peptides—Peptides (25 μg of GLUT1 in 50 μl of kaline) were resolved by reverse phase chromatography (30) using a polystyrene divinylbenzene copolymer column (5 μm, 300 Å, 150 $\times$ 2.1 mm; PLRP-S, Polymer Laboratories, Amherst, MA)) at 40 °C. Peptides were eluted using one of two gradients comprising solvent A (5% 1:1 (v/v) acetonitrile:isopropanol in water) and solvent B (1:1 (v/v) acetonitrile:isopropanol). Both solvents contained 0.1% formic acid and 0.01% trifluoroacetic acid (30, 31). Supernatant fractions were resolved using 15-min equilibration in 98% solvent A and 2% solvent B followed by raising the percentage of solvent B to 10% over 3 min, to 45% over 37 min, and to 95% over 2 min where it was held for 10 min prior to re-equilibration. The flow rate was 200 μl/min. Resolution of membrane fraction peptides required longer exposure to organic solvents: after 15 min of exposure to 95% solvent A and 5% solvent B, the percentage of solvent B was raised to 20% over 4 min and then to 95% over 56 min where it was held for 10 min prior to re-equilibration.

Electrospray Ionization Mass Spectrometry—ESI-MS analysis was performed using a Thermo Fisher LCQ or an LTQ electrospray ionization mass spectrometer. Operational parameters included positive ion mode; spray voltage, 4.5 kV; capillary temperature, 225 °C; and scan range, *m*/*z* 400–2,000. MS/MS

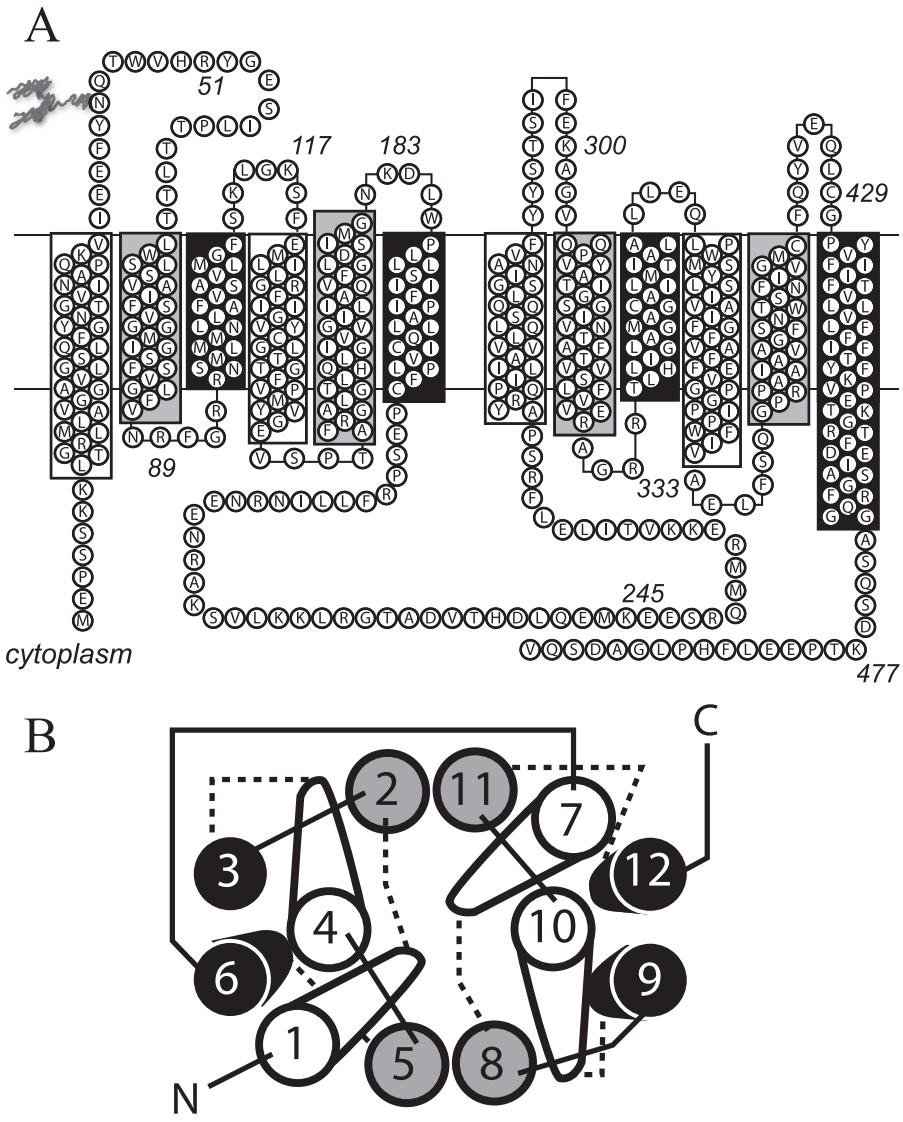

FIGURE 1. **Putative GLUT1 topology and helix packing.** *A*, GLUT1 topology adapted from the GlpT homology model (11). Group 1 TMs are highlighted in *white*. Group 2 and Group 3 TMs are highlighted in *gray* and *black*, respectively. Some TMs extend beyond the bilayer boundaries (indicated by *horizontal lines*). The bilayer-embedded region of TMs 1–12 comprise amino acids 17–39, 64–86, 93–112, 120–141, 157–178, 187–207, 267–291, 305–325, 335–356, 362–385, 401–421, and 431–452, respectively. GLUT1 is glycosylated at Asn^{45}. TMs 6 and 7 are linked by the large cytoplasmic loop (L6–7). *B*, putative helix packing arrangement viewed from the cytoplasmic surface. TMs are *numbered* and *colored* as in *A*. Cytoplasmic and exofacial loops are indicated by *solid* and *dashed lines*, respectively. The figure is adapted from Refs. 11, 13, and 14.

fragments of isolated peptide species were produced in the ion trap by collision-induced dissociation with helium gas at 35 V. Acquisition methods were created using Xcalibur (version 1.2). MS/MS spectra were identified using the Bioworks Sequest version 3.2 data base search program and the human red blood cell proteome data base compiled by Kakhniashvili *et al.* (32).

RESULTS

Experimental System—All experiments used GLUT1 proteoliposomes comprising purified GLUT1 and co-purified, native erythrocyte lipids. These proteoliposomes are unsealed and simultaneously expose endo- and exofacial GLUT1 domains to exogenous ligands, proteolytic enzymes, and antibodies (26, 33). All analyses were performed using untreated GLUT1 or GLUT1 exposed to trypsin or α-chymotrypsin for 2 h at 30 °C by which time proteolysis is complete as judged by SDS-PAGE or immunoblot analysis (29).

GLUT1 residues comprising individual TM α-helices, intra- and extracellular loops, and the N and C termini were assigned according to the homology model of Salas-Burgos *et al.* (11) (Fig. 1*A*) in which TMs are organized by location and function: those forming the aqueous translocation pathway (group 1 (TMs 1, 4, 7, and 10) and group 2 (TMs 2, 5, 8, and 11)) or those comprising the lipid bilayer-embedded scaffolding region (group 3 (TMs 3, 6, 9, and 12); Fig. 1*B* (13, 14)). Loops describe the TMs they connect. For example, L1–2 is the exofacial loop connecting TMs 1 and 2.

GLUT1 Accessibility to Proteolytic Enzymes—GLUT1 contains 35 potential tosylphenylalanyl chloromethyl ketone-treated trypsin proteolytic sites (16 lysine and 19 arginine residues (5)). These residues are located within proposed intra- and extracellular loops, within the N and C termini, and at the membrane/solvent interface. Our results show that 32 sites were detected by MS/MS analysis of trypsin-treated GLUT1 (Fig. 2*A*). Only residues Arg^{153} and Lys^{183} flanking TM5 and Lys^{451} at the C-terminal end of TM12 appear to be inaccessible to trypsin digestion.

α-Chymotrypsin is less specific and in our hands consistently cleaved GLUT1 at the C-terminal end of phenylalanine, tyrosine, tryptophan, leucine, alanine, methionine, and glutamic acid. These residues are located both in putative, water-exposed domains and in membrane-embedded protein domains. Each putative TM contains at least five potential α-chymotrypsin cleavage sites, but we observed TM-specific proteolysis (Fig. 2*B*). Although groups 1 and 2 TM α-chymotrypsin cleavage products were detected, group 3 TM proteolysis was not detected (Table 1 and Fig. 3*A*). The number of detected cleavage sites declined in the following order: group 1 (15 sites) > group 2 (10 sites) ≫ group 3 TMs (one site; see Table 1). Putative, extramembranous regions revealed more proteolytic products than membrane-embedded domains, and the longest contiguous regions of the protein (N and C termini, L1–2, and L6–7) produced twice as many cleavage products than shorter loops.

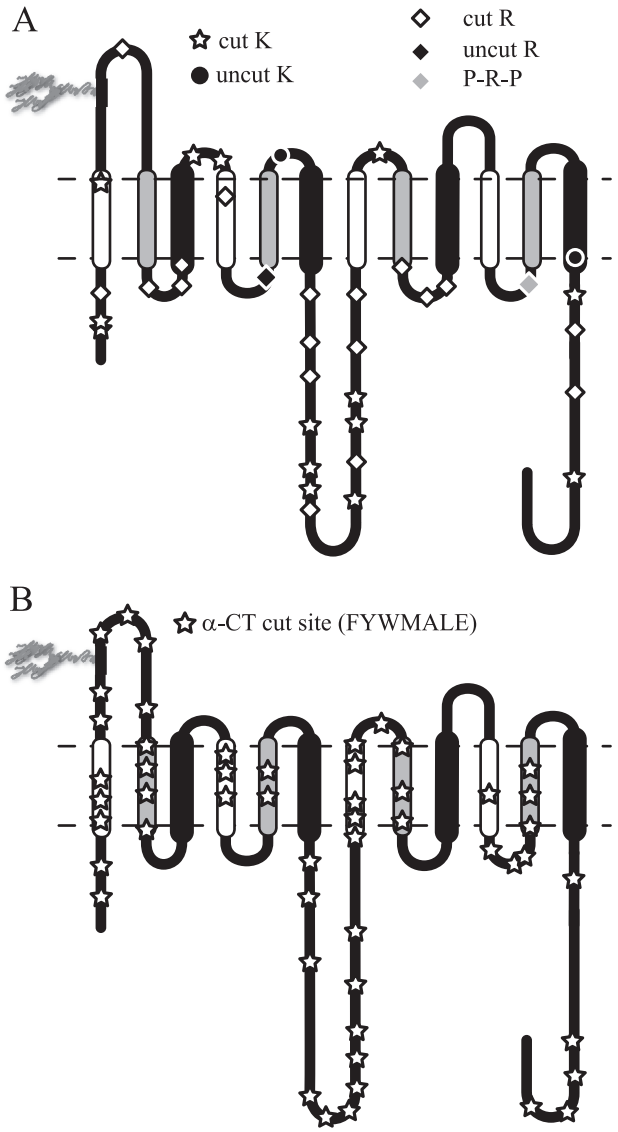

FIGURE 2. **Topography of protease-accessible sites.** Membrane-resident GLUT1 was digested with trypsin or α-chymotrypsin and then analyzed by reverse phase HPLC-ESI-MS/MS. Peptides containing the indicated cleavage sites were positively identified by MS/MS. *A*, GLUT1 contains 35 potential trypsin cleavage sites (16 lysine residues and 19 arginine residues). Thirty-two are cleaved by trypsin. ☆, observed lysine cleavage sites; ●, lysine residues not observed as cleavage sites; ◇, observed arginine cleavage sites; ◆, arginine residues not observed as cleavage sites. Arg^{400} (*gray* ◆) is flanked by N- and C-terminal proline residues and is not a potential trypsin cleavage site. *B*, GLUT1 contains 197 potential α-chymotrypsin cleavage sites (Phe, Tyr, Trp, Leu, Met, Ala, and Glu). The 52 detected cleavage sites are indicated by ☆. Potential α-chymotrypsin (*α-CT*) cleavage sites are present in all TM domains. TMs are *colored* as in Fig. 1.

TABLE 1
Susceptibility of GLUT1 side chains to proteolytic attack

Grouping and region[a]	Potential sites[b]	Sites cleaved[c]	Cleavage rate[d]	SSR[e]
			%	
1				
TM1	7	4	57	38.7
TM7	10	6	60	55.1
TM2	9	4	44	65.8
TM8	5	2	40	45.8
TM3	13	1	8	68.1
TM9	12	0	0	65.5
TM4	9	4	44	59.5
TM10	11	1	9	76.3
TM5	7	2	29	56.8
TM11	8	2	25	46.4
TM6	9	0	0	81.4
TM12	12	0	0	101.4
2				
Group 1 TMs (1, 4, 7, and 10)	37	15	41	57.4
Group 2 TMs (2, 5, 8, and 11)	29	10	34	53.7
Group 3 TMs (3, 6, 9, and 12)	46	1	2	79.1
3				
N terminus	10	5	50	
L1–2	10	7	70	44.1
L6–7	37	24	65	54.1
C terminus	19	10	53	37.5
Others	46	13	28	
Total	122	59	48	
4				
Membrane	112	26	23	
Extramembrane	122	59	48	
5				
GLUT1 total	234	85	36	

[a] Regions are delineated as 1) individual, membrane-embedded α-helices; 2) membrane-spanning helix groups; 3) loop, tail, and regions not embedded within the membrane; 4) summation of the individual membrane-embedded α-helices *versus* all other regions; and 5) the proteolytic susceptibility of the entire transport structure.
[b] The potential number of cleavage sites.
[c] The number of sites detected as cleavage sites.
[d] The percent accessibility of the region to proteolysis.
[e] The relative hydrophobicity of each region was calculated using the sequence specific retention (SSR) calculator developed by the Manitoba Center for Proteomics (42). For membrane-spanning α-helices, this calculation covers only peptide sequence that is embedded in the bilayer domain according to Salas-Burgos *et al.* (11) (Fig. 1).

SDS-PAGE-denatured GLUT1 was more uniformly accessible to protease (Fig. 3*B*). Residues Arg^{153} and Lys^{183} flanking TM5 were detected as tryptic cleavage sites in SDS-PAGE gel-eluted GLUT1. CD analysis demonstrated that gel-eluted GLUT1 contains significant α-helical structure, which may explain the persistent protease resistance of strongly hydrophobic TMs in the presence of SDS.

GLUT1 Peptide Water Solubility—GLUT1 proteolytic digests may be separated into membrane and aqueous fractions by centrifugation. Trypsin digestion released GLUT1 N and C termini, a portion of L1–2, and all of L6–7 into the aqueous buffer. The L1–2 peptide was detected only following GLUT1 deglycosylation by peptide-*N*-glycosidase F. Full-length TM1, cleaved at intracellular Arg^{11} and outer bilayer-hemileaflet Lys^{38}, was also detected in the aqueous fraction (Fig. 4*A*). α-Chymotrypsin digestion released a similar pattern of GLUT1 extramembranous regions into the aqueous fraction including the N and C termini, a portion of L7–8, and all of L1–2, L6–7, and L10–11. The isolated aqueous fraction also contained TM1 in its entirety as well as portions of TMs 2, 4, 7, 8, 10, and 11 (Fig. 4*B*).

TM8 (residues Ala^{301} through Arg^{330}) was released into the buffer when trypsin digestion was carried out in the presence of the transport inhibitor CB (10 μM; Figs. 4*A* and 5) or when the membrane fraction of a CB-free trypsin digest was resuspended in buffer containing CB. Cytochalasin D, DMSO, D-glucose, and maltose were unable to displace TM8 from trypsin-digested membranes. Dot-blots of α-chymotrypsin-digested GLUT1 using peptide-directed antibodies confirmed that GLUT1 N and C termini and loop 7–8 peptides were released by chymotrypsin but that loop 8–9 peptides (residues 325–338) were released only when CB was present during proteolysis.

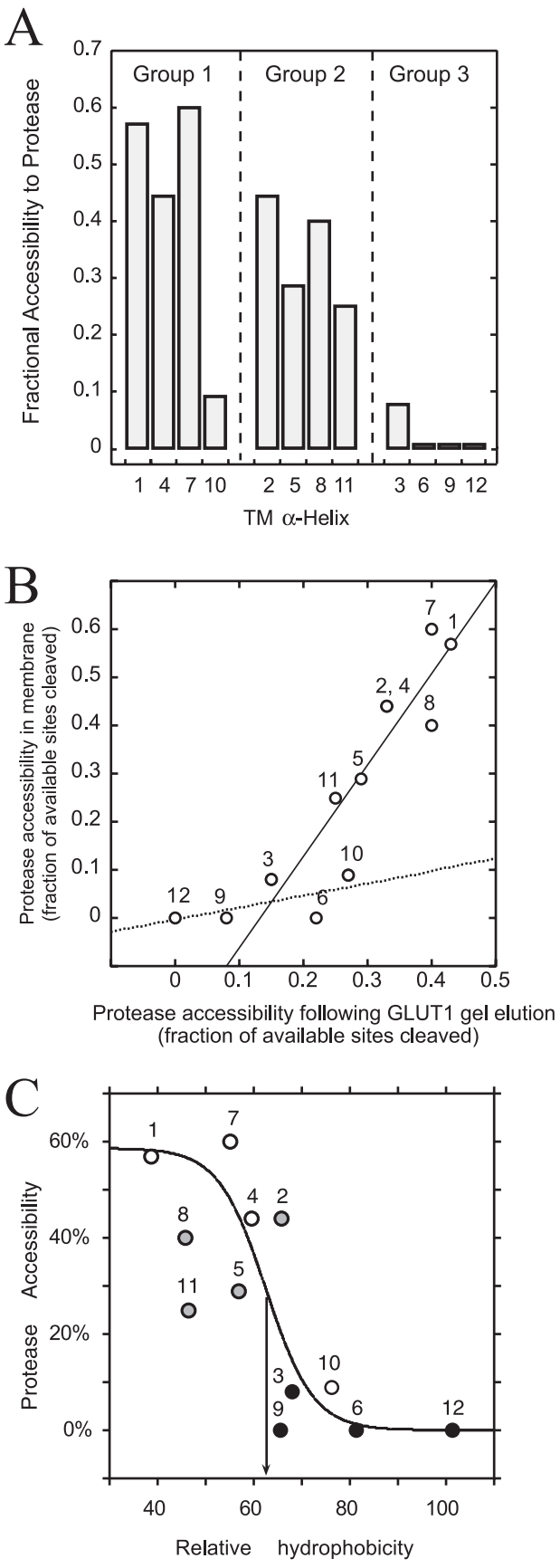

FIGURE 3. **Protease accessibility of bilayer-embedded TMs.** TMs are *colored* as in Fig. 1. *A*, GLUT1 TM protease accessibility (*ordinate*) arranged by TM number (*abscissa*) and group classification (*above* the *bars*). Accessibility is the ratio of experimentally observed to potential cleavage sites (trypsin and α-chymotrypsin). *B*, GLUT1 TM protease accessibility in membranes (*ordinate*, see *A*) *versus* GLUT1 TM protease accessibility following SDS-PAGE elution (*abscissa*). *Lines* were calculated by linear regression. The *solid line* is drawn through TMs 1, 2, 4, 5, 7, 8, and 11. The *dashed line* is drawn though TMs 3, 6, 9, 10, and 12. *C*, observed TM protease accessibility (*ordinate*) *versus* TM relative hydrophobicity (*abscissa*; calculated as sequence-specific retention score (42)). The *S-shaped curve* was obtained by nonlinear regression assuming protease accessibility (*P*) is related to TM hydrophobicity (*H*) through the logistic function $P = a/(1 + m \times n^{-H})$ where a, m, and n are 58.7 ± 15, (3.13 ± 0.14) × 10^{-6}, and 0.82 ± 0.09, respectively. The inflection point (*arrow*) occurs at 62.5% relative hydrophobicity. TMs are *numbered*.

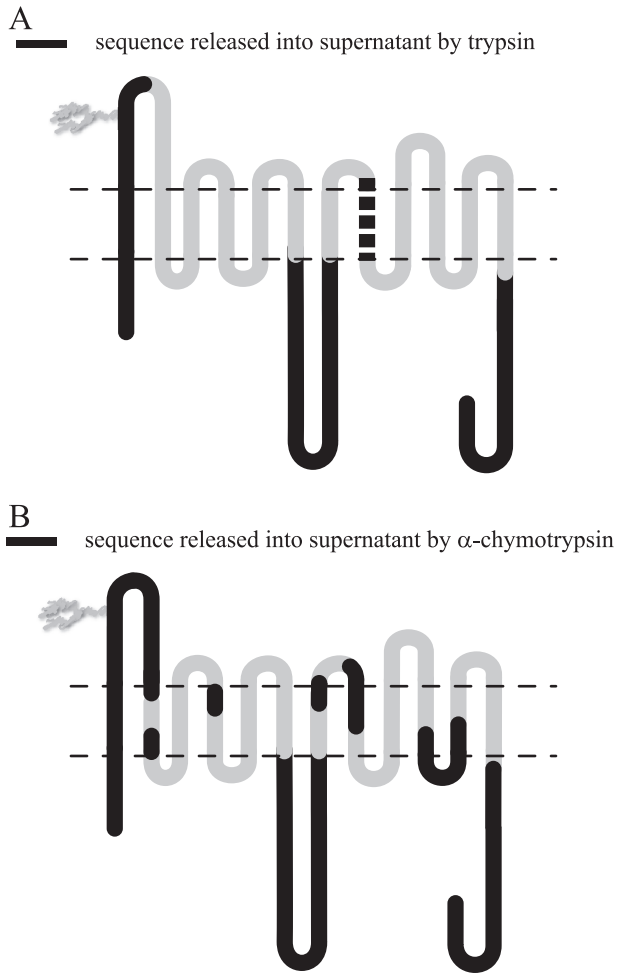

FIGURE 4. **GLUT1 peptides released into the aqueous environment.** Membrane-resident GLUT1 was digested with trypsin or α-chymotrypsin and sedimented, the aqueous fraction was collected, and its peptide content was identified by reverse phase HPLC-ESI-MS/MS. *A* and *B* show the GLUT1 membrane topology map of Fig. 1*A*. *Horizontal dashed lines* represent the membrane/water interface. Domains colored in *black* are detected in the aqueous fraction. *A*, trypsin digestion releases the N terminus, TM1 in its entirety (cut at Arg^{11} and Lys^{38}), a portion of L2, all of L6, and the C terminus. If CB (10 μM) is included during digestion or if the membrane pellet is resuspended in 10 μM CB, TM8 (cleaved at Lys^{300} and Arg^{330}; *thick dashed black line*) is released into the aqueous fraction. *B*, α-chymotrypsin-released fragments include the N terminus; TM1; L2; portions of TM2; TM4; all of L6; portions of TM7, TM8, TM10, L10, and TM11; and the C terminus.

Ligand Binding to Proteolyzed GLUT1—Trypsinization increased the CB binding capacity of GLUT1 (Table 2), increased $K_{d(app)}$ for CB binding, and decreased $K_{i(app)}$ for D-glucose inhibition of CB binding. Displacement of TM8 by trypsinization in the presence of 10 μM CB was without addi-

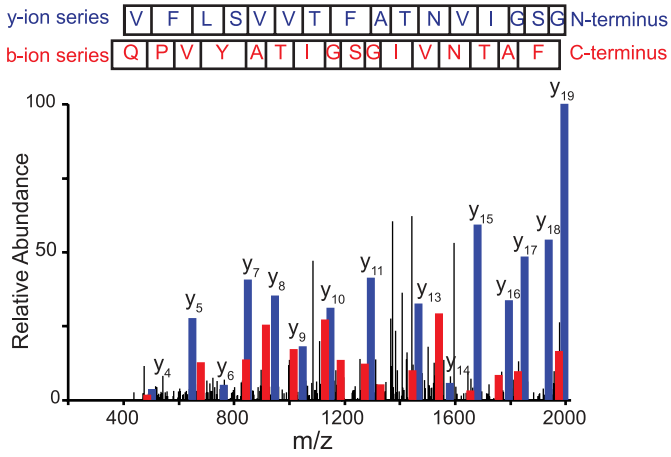

FIGURE 5. **MS/MS spectrum of CB-released TM8.** TM8 is released by CB during or following trypsin digestion. The peptide sequence is $K^{300} \downarrow$ AGVQQPVYATIGSGIVNTAFTVVSLFVVER$^{330} \downarrow$ A corresponding to L7–8 and TM8 at the membrane/cytoplasm interface (Fig. 1*A*). This peptide elutes from the HPLC column at 42.73 min (43% organic solvent). The indicated y- (read C to N terminus, *blue*) and b (read N to C terminus, *red*)-ion series confirm the identity of this peptide with the following Sequest scoring parameters: XCorr, 5.53, peptide probability, 7.43×10^{-8}; ΔCn, 0.75; and preliminary score, 1471.6.

TABLE 2
Ligand binding to GLUT1

Experiment[a]	Cytochalasin B binding[b]		D-Glucose binding[c]
	$K_{d(app)}$	B_{max}	$K_{i(app)}$
	nM	nM	mM
Control	133 ± 18	68 ± 9	8.6 ± 1.2
Post-trypsin	495 ± 80	118 ± 15	3.1 ± 0.5
Post-trypsin/CB	474 ± 73	119 ± 11	5.0 ± 0.8
α-Chymotrypsin	—	—	—

[a] [^{3}H]Cytochalasin B binding to GLUT1 proteoliposomes. CB binding was measured using GLUT1 proteoliposomes in saline buffer (control); GLUT1 proteoliposomes were incubated with trypsin to remove fragments L1, L2, L6, N and C termini, and TM1 (trypsin); GLUT1 was trypsinized in the presence of 10 μM CB to additionally remove TM8 (post-trypsin/CB); and GLUT1 proteoliposomes were treated with α-chymotrypsin. Results are shown as mean ± S.E. "—" indicates that CB binding was not detected.

[b] CB binding was measured in triplicate at 50–5000 nM CB. Two or more separate experiments were made per condition, and the entire data set was averaged for each [CB] in each condition. Binding displays simple Michaelis-Menten kinetics. Binding isotherms were analyzed by nonlinear regression to obtain the maximum binding and half-saturation constants (B_{max} and $K_{d(app)}$, respectively).

[c] Binding was also measured in the presence of D-glucose, a competitive inhibitor of CB binding to GLUT1 (19). $K_{i(app)}$ for D-glucose (Glc) inhibition of CB binding was calculated from *R*, the ratio (CB bound in the absence of Glc):(CB bound when Glc is present), as $K_{i(app)} = [Glc]/(((R(K_{d(app)} + [CB])) - [CB])/K_{d(app)} - 1)$.

tional impact on CB or D-glucose binding. CB binding to α-chymotrypsin-treated GLUT1 was undetectable (Table 2).

Covalent Modification of GLUT1 Residues—We examined covalent modification of GLUT1 lysine residues by the aqueous probe sulfo-NHS-LC-biotin, which reacts with the lysine primary amine side chain to form a covalent amide bond that withstands MS/MS ionization. Studies with isothiocyanates (fluorescein isothiocyanate and phenylisothiocyanate) demonstrate sugar and CB modification of probe incorporation, but these probes, although detected in ESI time-of-flight analyses, were not detected by MS/MS suggesting that they do not withstand MS/MS ionization.

GLUT1 modification by sulfo-NHS-LC-biotin is a second order reaction as evidenced by the linear dependence of the pseudo-first-order constant for GLUT1 modification on [sulfo-NHS-LC-biotin] at fixed [GLUT1] (Fig. 6, *A* and *B*). The extent of modification became saturated at probe to protein ratios above 200:1 and was half-maximal at a probe to protein ratio of 15.5 ± 3.2:1 (Fig. 6*B*). Biotin incorporation, as judged by ELISA analysis of biotinylated bovine serum albumin as a standard, became saturated at 4.3 mol of biotin/mol of GLUT1. GLUT1 modification by sulfo-NHS-biotin (spacer arm = 13.5 Å) was significantly less (as judged by ELISA) than GLUT1 modification by sulfo-NHS-LC-biotin (spacer arm = 22.4 Å; data not shown).

Maltose and D-glucose (50 mM) increased maximum GLUT1 biotinylation by 19 ± 4 and 33 ± 4%, respectively ($n = 3$), whereas CB (10 μM) was without effect on GLUT1 biotinylation ($n = 3$). GLUT1 CB binding capacity was unchanged by GLUT1 biotinylation, but GLUT1 affinity for CB was reduced with half-maximal inhibition at a probe to protein ratio of 43 ± 17:1 (Fig. 6*C*). Modified GLUT1 peptides were identified by searching for the expected 339.16-Da lysine adduct using the Sequest analysis program. Comparison of MS/MS spectra for unmodified (Fig. 7*A*) and modified (Fig. 7*B*) GLUT1 peptides containing Lys^{245} showed how the *m*/*z* ratio differs in the b- and y-ion series peaks that correspond to the unlabeled or labeled lysine. Cytoplasmic lysine residues in L6–7 and the C terminus are equally accessible to NHS ester at probe:protein ratios of 20:1 and 200:1 (Table 3 and Ref. 30).

Table 3 summarizes the putative locations, susceptibility to trypsin proteolysis, and accessibility to covalent modification of GLUT1 lysine residues. Of the 14 trypsin-accessible GLUT1 lysine residues, 12 were detected as biotinylated products. Lys^{114} of extracellular L3–4 and Lys^{456} at the C-terminal end of TM12 were not detected as labeled amino acids. This could mean that these sites are not modified or that modification blocks trypsin cleavage and subsequently prevents production and detection of these peptides by MS/MS.

Alkylation of membrane-resident, non-reduced GLUT1 using iodoacetamide yielded alkylated cysteine residues at positions Cys^{133}, Cys^{201}, and Cys^{429}. GLUT1 reduction prior to alkylation also yielded alkylated Cys^{207} and Cys^{421}. GLUT1 cysteine Cys^{347} was neither detected as an alkylated or unmodified residue but was detected as an acrylamide-modified residue in digested, gel-eluted, SDS-denatured, reduced GLUT1.

DISCUSSION

This study represents the first extensive analysis of GLUT1 structure by chemical footprinting. Our goal was to map membrane-resident GLUT1 accessibility to aqueous probes. Our findings provide new insights into the role of specific membrane-spanning helices in GLUT1 conformational states and indicate that modeled GLUT1 topology requires some adjustment.

GLUT1 proteoliposome trypsinization revealed the following. 1) Proteolysis is complete within 2 h. 2) Thirty-two of 35 possible tryptic cleavage sites are accessible to trypsin. 3) SDS denaturation exposes two of the three resistant cleavage sites. 4) Trypsin-treated GLUT1 retains D-glucose binding affinity and twice the ligand (CB) binding capacity of nonproteolyzed GLUT1. 5) Proposed water-exposed loops (loops 1–2 and 6–7 and the C terminus) are released into the aqueous buffer. 6)

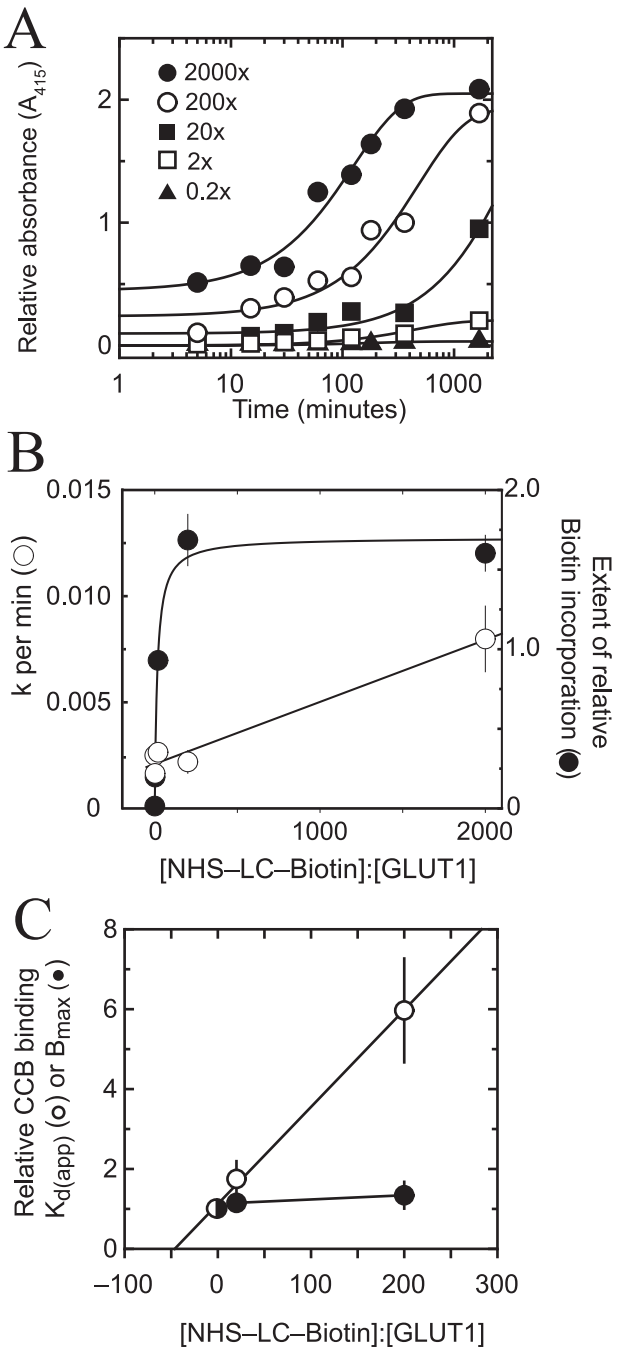

FIGURE 6. **GLUT1 modification by sulfo-NHS-LC-biotin.** *A*, time course of GLUT1 labeling at 20 °C. Each data point represents the mean ± S.E. of at least four separate measurements. Curves were computed by nonlinear regression assuming pseudo-first-order kinetics described by the following: labeling = $B_0 + B_\infty(1 - e^{-k \cdot t})$. *B*, the results of *A* are plotted as the rate of GLUT1 modification (k, ○) *versus* the probe to protein molar ratio or as the maximum extent of GLUT1 modification (B_∞, ●) *versus* the probe to protein molar ratio. Curves were calculated by nonlinear regression. The rate of labeling increases linearly with [probe] and is described by rate = $(2.92 \times 10^{-6} \pm 0.30 \times 10^{-6})$[probe] + $(0.0021 \pm 0.0003\ \text{min}^{-1})$, $R^2 = 0.984$. The extent of labeling increases in a saturable fashion with [probe] and is described by $B_{max} = 1.70 \pm 0.06$ and $K_{1/2} = 15.5 \pm 3.2$:1, $\chi^2 = 1.9 \times 10^{-2}$. *C*, effect of GLUT1 biotinylation on GLUT1 CB binding. *Ordinate*, biotinylated GLUT1 CB binding capacity (●) or $K_{d(app)}$ (○) relative to untreated GLUT1; *abscissa*, NHS-LC-biotin:GLUT1 molar ratio. Results are shown as mean ± S.E. of three experiments made in quadruplicate. For control GLUT1, $B_{max} = 0.45 \pm 0.01$ mol of CB/mol of GLUT1 and $K_{d(app)} = 265 \pm 16$ nM. The line through the $K_{d(app)}$ data was computed by linear regression and extrapolates on the *abscissa* to a probe to protein molar ratio of −43 ± 17.

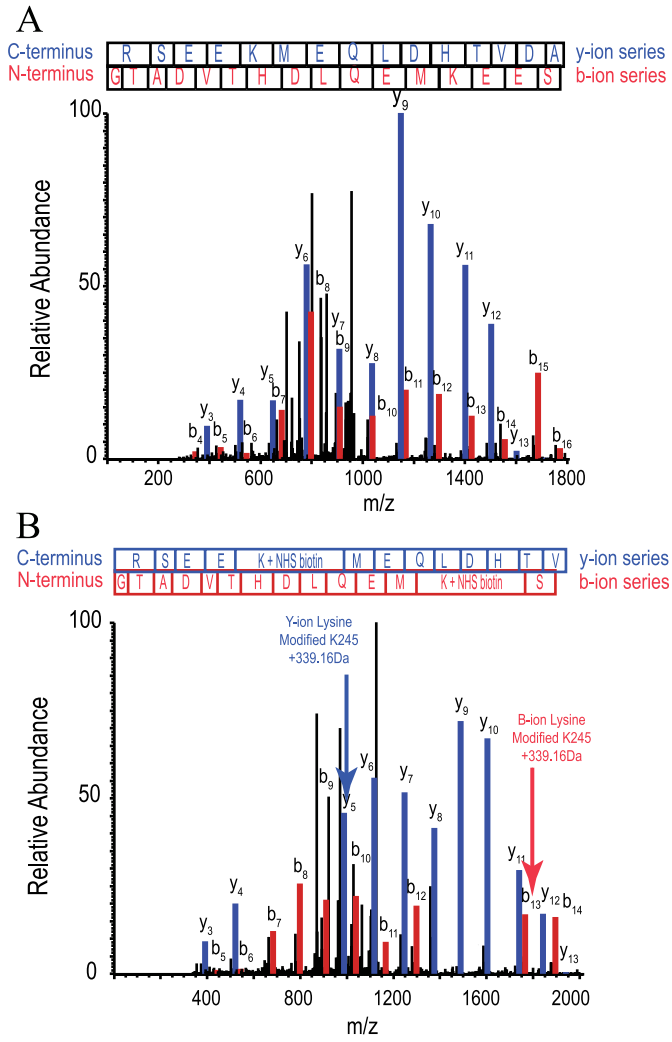

FIGURE 7. **MS/MS spectra of a GLUT1 peptide modified by sulfo-NHS-LC-biotin.** Sulfo-NHS-LC-biotin covalently modifies lysine side chain primary amines producing a covalent mass addition of 339.16 Da. *A*, MS/MS spectrum of a GLUT1 tryptic peptide $R^{232} \downarrow$ GTADVTHDLQEMKEESR$^{249} \downarrow$ Q from L6–7. The peptide elutes at 10.47 min (26% organic solvent). The y- and b-ion series (*blue* and *red*, respectively) confirm the identity of the unmodified peptide with Sequest scoring parameters as follows: XCorr, 4.636; peptide probability, 3.4×10^{-9}; ΔCn, 0.740; and preliminary score, 1975.5. *B*, the same peptide, except modified at Lys^{245} by sulfo-NHS-LC-biotin. Modification is first observed at y_5 and b_{13}, which show a 339.16-Da lysine adduct. All sequential ions in each series show this mass adduct. The modified peptide elutes at 19.64 min (31% organic solvent). The MS/MS spectrum and Sequest scoring parameters confirm its identity (XCorr, 4.652; peptide probability, 5×10^{-9}; ΔCn, 0.615; and preliminary score, 1235.2

Putative TM1 is released into the aqueous buffer. 7) Putative TM8 is retained until GLUT1 interacts with CB whereupon TM8 is also released from the membrane.

GLUT1 covalent modification by sulfo-NHS-LC-biotin indicated the following. 1) GLUT1 is modified only at lysine residues. 2) Modification kinetics are second order. 3) Each GLUT1 molecule incorporates a maximum of 4.3 molecules of biotin. 4) Twelve of 16 potential biotinylation sites are detected as modified lysine residues by MS/MS. 5) Biotinylated GLUT1 retains CB binding capacity but loses affinity for CB with increasing biotinylation. These results suggest that GLUT1 biotinylation is underestimated by the ELISA assay or that biotinylation is stochastic and progressively autoinhibitory. Reduced GLUT1

TABLE 3
Accessibility of GLUT1 lysine residues to covalent modification

Lysine residue[a]	Putative location[b]	Detected as labeled,[c] [NHS-LC-biotin]:[GLUT1]			Detected as cleaved[d]
		2:1	20:1	200:1	
Lys^{6}	N terminus	—	Yes	Yes	Yes
Lys^{7}	TM1	—	Yes	Yes	Yes
Lys^{38}	TM1	—	—	Yes	Yes
Lys^{114}	L3–4	—	—	—	Yes
Lys^{117}	L3–4	—	—	Yes	Yes
Lys^{183}	L5–6	—	—	—	—
Lys^{225}	L6–7	Yes	Yes	Yes	Yes
Lys^{229}	L6–7	Yes	Yes	Yes	Yes
Lys^{230}	L6–7	Yes	Yes	Yes	Yes
Lys^{245}	L6–7	Yes	Yes	Yes	Yes
Lys^{255}	L6–7	Yes	Yes	Yes	Yes
Lys^{256}	L6–7	Yes	Yes	Yes	Yes
Lys^{300}	L7–8	—	Yes	Yes	Yes
Lys^{451}	TM12	—	—	—	—
Lys^{456}	C terminus	—	—	—	Yes
Lys^{477}	C terminus	Yes	Yes	Yes	Yes

[a] GLUT1 lysine residues.
[b] Their location within GLUT1 putative domains.
[c] Their biotinylation by sulfo-NHS-LC-biotin as detected by MS/MS (at the three molar ratios of sulfo-NHS-LC-biotin:GLUT1. "Yes" indicates that the modified residue was observed; "—" indicates that the modified residue is not detected.
[d] Their propensity to cleavage by trypsin as detected by MS/MS.

labeling by sulfo-NHS-biotin (spacer arm = 13.5 Å) relative to modification by sulfo-NHS-LC-biotin (spacer arm = 22.4 Å) suggests that quantitation of biotinylation by ELISA is limited by accessibility to horseradish peroxidase-streptavidin.

Thirty-two lysine and arginine residues were accessible to aqueous probes supporting their proposed assignment to GLUT1 extramembranous regions. Arg^{153}, Lys^{183}, and Lys^{451} were not detected as tryptic cleavage sites. Lys^{114}, Lys^{183}, Lys^{451}, and Lys^{456} were not detected as sulfo-NHS-LC-biotin-reactive sites. These results suggest that Arg^{153}, Lys^{183}, and Lys^{451} are inaccessible to polar probes.

TM5 adjustment to relocate putative cytoplasmic (but trypsin-inaccessible) Arg^{153} to the cytoplasm/membrane interface (a translation of six residues toward the interstitium) also relocates Lys^{183} of exofacial loop 5–6 to the interstitium/membrane junction of TM6. This explains the trypsin and/or NHS ester inaccessibility of Arg^{153} and Lys^{183} (this study), the unexpected accessibility of mutants Q161C and I164C of TM5 to interstitial 4-(chloromercuri)benzosulfonic acid (10), and the SDS-dependent accessibility of Arg^{153} and Lys^{183} (this study).

TM12 adjustment to relocate Lys^{451} one additional helix turn into the lipid bilayer (direction cytoplasm to interstitium) would explain the trypsin inaccessibility of Lys^{451} (this study) and, by displacing N-terminal TM12 sequence into the interstitium, may also explain the unexpected accessibility of TM12 Y432C through I436C to interstitial 4-(chloromercuri)benzosulfonic acid (10). These interpretations must be tempered by the possibility of residue occlusion by local structure. The significant α-chymotrypsin resistance of TMs 3, 6, 9, and 12 is consistent with the hypothesis that these TMs are the most hydrophobic and most closely associated with the membrane bilayer.

The GLUT1/GlpT homology model does not address the suggested roles of Cys^{347} (in TM9) and Cys^{421} (TM11) in promoting GLUT1 oligomerization in mammalian cells (23, 27, 34). The present study confirmed that Cys^{421} in TM11 is available for alkylation only following GLUT1 reduction and that modification of Cys^{347} requires GLUT1 reduction and denaturation.

The present study indicated that CB and D-glucose binding do not require intact GLUT1 N and C termini, L1–2, L2–3, L6–7, TM1, or TM8. GLUT1 CB binding is lost following α-chymotrypsin digestion suggesting that the loss of loop 10–11 and/or more extensive proteolysis eliminates binding. These observations are consistent with the suggested role of L10–11 in CB binding (35) and argue against the role of L2–3 suggested by docking simulations (11). Trypsin-dependent increased GLUT1 CB binding capacity is consistent with previous reports of trypsin-induced uncoupling of GLUT1 oligomers that normally present only one CB binding site for every two GLUT1 subunits (36).

Mueckler and Makepeace (see Ref. 10 to review this extensive body of work) show by scanning cysteine mutagenesis that GLUT1 α-helices are amphipathic and vary in accessibility to interstitial polar molecules. Except for TMs 4 and 12, the examined TMs show solvent accessibility predicted by the MFS helix-packing model.

The alternating conformer hypothesis for carrier-mediated transport (37) proposes that uniporters isomerize between export (e1) and import (e2) conformers in the absence and presence of substrate. Membrane-spanning helices that undergo reorganization during the GLUT1 transport cycle have not been identified. The present study sheds new light on this question.

Trypsinolysis cut TMs 1, 2, 3, 7, and 8 at N and C termini thereby isolating each TM from the remaining intact membrane domains (Fig. 2*A*). Reverse phase chromatography demonstrated that the hydrophilicity of these TMs follows the order 1 > 8 > 7 > 2 > 3 (Fig. 3). Only TMs 1 and 8 were released into buffer indicating that each is poised at the limits of membrane solubility and is constrained only by the intact polypeptide backbone. TM1 was released in the absence of substrate. CB (but not D-glucose) promoted TM8 release from trypsinized GLUT1 indicating that TM8 is unstable only in the GLUT1-CB complex. CB binding also promotes GLUT1 proteolysis by thermolysin at a cytoplasmic, C-terminal site in TM7 (19). Our previous studies have demonstrated that the combination of GLUT1 trypsinization and exposure to cytochalasin B promotes sugar occlusion within the GLUT1 translocation pathway (38). Thus, although the metastable association of TMs 1 and 8 with the GLUT1 TM scaffold exerts only a minor influence on GLUT1 ligand binding affinity, the release of these TMs from the scaffold stabilizes a GLUT1-sugar translocation intermediate. TMs 1 and 8 may act to destabilize the translocation intermediate and thereby accelerate sugar translocation.

The ligand-coordinating domains of GLUT1 are only poorly defined. Disaccharide binding to LacY involves TMs 1, 4, 5, 7, 8, and 11 (13). TMs coordinating glycerol phosphate binding to GlpT are proposed to include TMs 1 and 7 (14). Homology modeling suggests involvement of GLUT1 TMs 2, 4, 5, 7, 8, and 10 in substrate binding (11), although caveats with this approach have been noted (22). Scanning cysteine mutagenesis implicates GLUT1 TMs 1, 5, 7, 8, and 11 in sugar binding (10).

CB interacts with a GLUT1 region comprising residues Trp^{388} through Trp^{412} (19), which form the cytoplasmic loop and TM segments of the TM10-TM11 hairpin (11).

GLUT1 behavior is strikingly similar to that of the α subunit of the primary active carrier Na,K-ATPase. The Na,K-ATPase TM5-TM6 hairpin is released following trypsinolysis, but release is prevented by the pump inhibitor ouabain or by Rb occlusion (39). P1 ATPase crystal structures reveal that the TM5-TM6 hairpin forms the major cation binding site of this family of primary active carriers (40, 41). Thus an amphipathic region of an e1•e2 primary active carrier undergoes conformational change upon ligand binding and is released from the carrier scaffold only in the absence of substrate. Modeled GLUT1 (a *passive* e1•e2 carrier) reveals at least 13 and 16 helix-helix contacts between TMs 8 and 10 and TMs 7 and 10, respectively (11). We propose that TM10 displacement upon CB/TM10-TM11 hairpin interaction alters TM8/TM10 and TM7/TM10 associations causing TM8 release from the membrane and TM7 partial displacement into cytosol where it becomes thermolysin-accessible. TM1 is only weakly associated with the GLUT1 TM scaffold, and its release into solvent water reveals the inherently amphipathic character, aqueous exposure, and metastability of translocation pathway-forming TMs.

CONCLUSIONS

We observed close correspondence between experimental and proposed GLUT1 membrane topographies. The locations of TMs 5, 6, and 12 require small adjustments to account for solvent inaccessibility of Arg^{153}, Lys^{183}, and Lys^{451}. An unanticipated result was the concurrence between the hydrophilicity of GLUT1 putative membrane-spanning α-helices and their experimental *in situ* accessibility to α-chymotrypsin. TMs 1 and 8 are poised at the limits of bilayer solubility, are released into the aqueous medium upon GLUT1 trypsinization (TM1) or subsequent addition (TM8) of ligand, illustrate the intrinsically metastable organization of translocation pathway TMs within the carrier scaffold, and may serve to destabilize a transport cycle intermediate in which sugar becomes occluded within the translocation pathway.

REFERENCES

1. Saier, M. H., Jr., Beatty, J. T., Goffeau, A., Harley, K. T., Heijne, W. H., Huang, S. C., Jack, D. L., Jahn, P. S., Lew, K., Liu, J., Pao, S. S., Paulsen, I. T., Tseng, T. T., and Virk, P. S. (1999) *J. Mol. Microbiol. Biotechnol.* **1,** 257–279
2. Joost, H. G., Bell, G. I., Best, J. D., Birnbaum, M. J., Charron, M. J., Chen, Y. T., Doege, H., James, D. E., Lodish, H. F., Moley, K. H., Moley, J. F., Mueckler, M., Rogers, S., Schurmann, A., Seino, S., and Thorens, B. (2002) *Am. J. Physiol.* **282,** E974–E976
3. Joost, H. G., and Thorens, B. (2001) *Mol. Membr. Biol.* **18,** 247–256
4. Guo, X., Geng, M., and Du, G. (2005) *Biochem. Genet.* **43,** 175–187
5. Mueckler, M., Caruso, C., Baldwin, S. A., Panico, M., Blench, I., Morris, H. R., Allard, W. J., Lienhard, G. E., and Lodish, H. F. (1985) *Science* **229,** 941–945
6. Cairns, M. T., Alvarez, J., Panico, M., Gibbs, A. F., Morris, H. R., Chapman, D., and Baldwin, S. A. (1987) *Biochim. Biophys. Acta* **905,** 295–310
7. Hresko, R. C., Kruse, M., Strube, M., and Mueckler, M. (1994) *J. Biol. Chem.* **269,** 20482–20488
8. Hruz, P. W., and Mueckler, M. M. (2001) *Mol. Membr. Biol.* **18,** 183–193
9. Jung, E. K., Chin, J. J., and Jung, C. Y. (1986) *J. Biol. Chem.* **261,** 9155–9160
10. Mueckler, M., and Makepeace, C. (2006) *J. Biol. Chem.* **281,** 36993–36998
11. Salas-Burgos, A., Iserovich, P., Zuniga, F., Vera, J. C., and Fischbarg, J. (2004) *Biophys. J.* **87,** 2990–2999
12. Dahl, S. G., Sylte, I., and Ravna, A. W. (2004) *J. Pharmacol. Exp. Ther.* **309,** 853–860
13. Abramson, J., Smirnova, I., Kasho, V., Verner, G., Kaback, H. R., and Iwata, S. (2003) *Science* **301,** 610–615
14. Huang, Y., Lemieux, M. J., Song, J., Auer, M., and Wang, D. N. (2003) *Science* **301,** 616–620
15. Yin, Y., He, X., Szewczyk, P., Nguyen, T., and Chang, G. (2006) *Science* **312,** 741–744
16. Hirai, T., Heymann, J. A., Shi, D., Sarker, R., Maloney, P. C., and Subramaniam, S. (2002) *Nat. Struct. Biol.* **9,** 597–600
17. Kasho, V. N., Smirnova, I. N., and Kaback, H. R. (2006) *J. Mol. Biol.* **358,** 1060–1070
18. Holyoake, J., Caulfeild, V., Baldwin, S. A., and Sansom, M. S. (2006) *Biophys. J.* **91,** L84–L86
19. Holman, G. D., and Rees, W. D. (1987) *Biochim. Biophys. Acta* **897,** 395–405
20. Inukai, K., Asano, T., Katagiri, H., Anai, M., Funaki, M., Ishihara, H., Tsukuda, K., Kikuchi, M., Yazaki, Y., and Oka, Y. (1994) *Biochem. J.* **302,** 355–361
21. Garcia, J. C., Strube, M., Leingang, K., Keller, K., and Mueckler, M. M. (1992) *J. Biol. Chem.* **267,** 7770–7776
22. Lemieux, M. J. (2007) *Mol. Membr. Biol.* **24,** 333–341
23. Graybill, C., van Hoek, A. N., Desai, D., Carruthers, A. M., and Carruthers, A. (2006) *Biochemistry* **45,** 8096–8107
24. Hebert, D. N., and Carruthers, A. (1992) *J. Biol. Chem.* **267,** 23829–23838
25. Steck, T. L., and Yu, J. (1973) *J. Supramol. Struct.* **1,** 220–232
26. Sultzman, L. A., and Carruthers, A. (1999) *Biochemistry* **38,** 6640–6650
27. Zottola, R. J., Cloherty, E. K., Coderre, P. E., Hansen, A., Hebert, D. N., and Carruthers, A. (1995) *Biochemistry* **34,** 9734–9747
28. Laemmli, U. K. (1970) *Nature* **227,** 680–685
29. Blodgett, D. M., De Zutter, J. K., Levine, K. B., Karim, P., and Carruthers, A. (2007) *J. Gen. Physiol.* **130,** 157–168
30. Weinglass, A., Whitelegge, J. P., Faull, K. F., and Kaback, H. R. (2004) *J. Biol. Chem.* **279,** 41858–41865
31. Abe, Y., Chaen, T., Jin, X. R., Hamasaki, T., and Hamasaki, N. (2004) *J. Biochem.* (*Tokyo*) **136,** 97–106
32. Kakhniashvili, D. G., Bulla, L. A. J., and Goodman, S. R. (2004) *Mol. Cell. Proteomics* **3,** 501–509
33. Appleman, J. R., and Lienhard, G. E. (1989) *Biochemistry* **28,** 8221–8227
34. Levine, K. B., Cloherty, E. K., Hamill, S., and Carruthers, A. (2002) *Biochemistry* **41,** 12629–12638
35. Karim, A. R., Rees, W. D., and Holman, G. D. (1987) *Biochim. Biophys. Acta* **902,** 402–405
36. Coderre, P. E., Cloherty, E. K., Zottola, R. J., and Carruthers, A. (1995) *Biochemistry* **34,** 9762–9773
37. Jardetzky, O. (1966) *Nature* **211,** 969–970
38. Blodgett, D. M., and Carruthers, A. (2005) *Biochemistry* **44,** 2650–2660
39. Lutsenko, S., Anderko, R., and Kaplan, J. H. (1995) *Proc. Natl. Acad. Sci. U. S. A.* **92,** 7936–7940
40. Olesen, C., Picard, M., Winther, A. M., Gyrup, C., Morth, J. P., Oxvig, C., Moller, J. V., and Nissen, P. (2007) *Nature* **450,** 1036–1042
41. Morth, J. P., Pedersen, B. P., Toustrup-Jensen, M. S., Sorensen, T. L., Petersen, J., Andersen, J. P., Vilsen, B., and Nissen, P. (2007) *Nature* **450,** 1043–1049
42. Krokhin, O. V., Craig, R., Spicer, V., Ens, W., Standing, K. G., Beavis, R. C., and Wilkins, J. A. (2004) *Mol. Cell. Proteomics* **3,** 908–919